Electrochemistry of Conductive Polymers 39. Contacts between Conducting Polymers and Noble Metal Nanoparticles Studied by Current-Sensing Atomic Force Microscopy

Shin Hyo Cho and Su-Moon Park*

Department of Chemistry and Center for Integrated Molecular Systems, Pohang University of Science and Technology, Pohang, Gyeongbuk 790-784, Republic of Korea

Received: September 1, 2006; In Final Form: October 11, 2006

Electrical properties of contacts formed between conducting polymers and noble metal nanoparticles have been examined using current-sensing atomic force microscopy (CS-AFM). Contacts formed between electrochemically prepared π-conjugated polymer films such as polypyrrole (PPy), poly(3-methylthiophene) (P3MeT), as well as poly(3,4-ethylenedioxythiophene) (PEDOT) and noble metal nanoparticles including platinum (Pt), gold (Au), and silver (Ag) have been examined. The Pt nanoparticles were electrochemically deposited on a pre-coated PPy film surface by reducing a platinum precursor ($PtCl_6^{2-}$) at a constant potential. Both current and scanning electron microscopic images of the film showed the presence of Pt islands. The Au and Ag nanoparticles were dispersed on the P3MeT and PEDOT film surfaces simply by dipping the polymer films into colloid solutions containing Au or Ag particles for specified periods (5 to ~10 min). The deposition of Au or Ag particles resulted from either their physical adsorption or chemical bonding between particles and the polymer surface depending on the polymer. When compared with PPy, P3MeT and PEDOT showed a stronger binding to Au or Ag nanoparticles when dipped in their colloidal solutions for the same period. This indicates that Au and Ag particles are predominantly linked with the sulfur atoms via chemical bonding. Of the two, PEDOT was more conductive at the sites where the particles are connected to the polymer. It appears that PEDOT has better aligned sulfur atoms on the surface and is strongly bonded to Au and Ag nanoparticles due to their strong affinity to gold and silver. The current−voltage curves obtained at the metal islands demonstrate that the contacts between these metal islands and polymers are ohmic.

Introduction

Recently, devices fabricated using molecular and nanometer scale materials such as single molecules,[1] supramolecules,[2] carbon nanotubes,[3] self-assembled monolayers,[4] and conducting polymers[5] have been studied extensively as electronic circuit elements owing to their potential applications to electronic devices.[6] For the construction of electronic circuits on a molecular or nanoscale level, however, there are a number of problems that need to be addressed. One of the main problems is the nature of electrical contacts between the individual molecules or the molecular assemblies and the metal leads. Unless well-defined and robust electrical contacts are made, it is difficult to obtain correct current−voltage responses for bulk conducting polymer films, nanodots, or nanowires, which would be essential requirements for constructing electronic devices. Thus, establishing the nature of the electrical contact is a key requirement in the development of molecular electronic devices,[7] and characterization of their electronic transport properties across the contacts should be preceded. The nature of the contact is also critical to the electrocatalysis work, in which conducting polymers serve as conducting substrates for catalysis by noble metal nanoparticles such as those of platinum, iridium, etc.[8]

Current-sensing atomic force microscopy (CS-AFM) using a conductive probe, also named conducting probe AFM (CP-AFM), is a good tool for characterization for these purposes because the technique allows an easy and reproducible contact to be established with a variety of substances under precisely controlled load forces between the tip and the sample.[9] This modified AFM technique allows not only two-dimensional topographic and current images to be obtained simultaneously but also current−voltage characteristics to be measured at selected points of the image. Thus, electronic transport properties at various materials including single molecules,[10] self-assembled monolayers,[11] carbon nanotubes,[12] quantum dots,[13] and others[14] have been studied by measuring current−voltage traces. CS-AFM was also successfully applied to the investigation of electrochemically prepared conducting polymers including polyaniline,[15] polypyrrole,[16] and poly(3-methylthiophene) derivatives[17] showing its utility for nanoscopic examinations of conducting polymers.

Nanocomposites can be prepared from a range of different metals and conjugated polymers as well as oligomer linkers and have received considerable attention owing to the possibilities of creating suitable materials for electrocatalysis, chemical sensors, and microelectronics.[18] The composites can be prepared by electrochemical and chemical methods. The electrochemical method is a well-established technique that has been used widely for the preparation of conducting polymer films[19] as well as their nanocomposites with metal particles.[20] A recent review describes the preparation of nanocomposites of metal nanoparticles and conducting polymers as well as their electronic and optical properties.[20]

In the present paper, we report the spontaneous deposition of Au and Ag nanoparticles on sulfur containing conducting polymer surfaces by simply dipping the polymer films into colloid solutions containing these particles for a specified

* Corresponding author. E-mail: smpark@postech.edu; phone: +82-54-279-2102; fax: +82-54-279-3399.

10.1021/jp0656781 CCC: $33.50
Published on Web 11/30/2006

duration. This is an extremely simple procedure to form a metal-conducting polymer bonding through chemical bonding without using any linkers. Also, the electrochemical technique was shown to make good physical contacts with the polymer surface. We report electronic transport characteristics of these contacts studied by CS-AFM.

Experimental Procedures

Chemicals. Acetonitrile (ACN, Aldrich, 99.8%, anhydrous), propylene carbonate (PC, Aldrich 99.8%, anhydrous), sodium dodecyl sulfate (SDS, Fluka, 99%), 3-methylthiophene (3MeT: Aldrich, 98%), 3,4-ethylenedioxythiophene (EDOT, Aldrich), potassium hexachloroplatinate (K_2PtCl_6, Kojima, 99%), gold colloids (20 nm, Sigma), silver perchlorate ($AgClO_4$, Aldrich, 99.9%), and sodium borohydride ($NaBH_4$, Aldrich, 98%) were used as received. Lithium perchlorate ($LiClO_4$, Aldrich, 99.99%) was used after drying in a vacuum oven at 110 °C for 16 h. Pyrrole (Aldrich, 98%) was used after distillation over zinc powder and stored in the dark under a nitrogen atmosphere.

Electrochemical Experiments. All electrochemical experiments were carried out employing an EG&G Princeton Applied Research model 273A potentiostat/galvanostat controlled by a computer. An electrochemical cell with a three-electrode configuration was used for all electrochemical experiments. Gold-on-silicon (with Cr adhesive layers, Inosteck) and glassy carbon (for energy dispersive X-ray (EDX) analysis) were used as working electrodes (diameter: 5.7 mm). The gold-on-silicon electrode was annealed for 10 min with a hydrogen flame after they had been cleaned in a piranha solution (H_2SO_4/H_2O_2 = 70:30 v/v) and rinsed with deionized water. A piece of platinum gauze and a silver wire were used as counter and pseudo-reference electrodes, respectively, in nonaqueous media. In aqueous media, an Ag/AgCl (in saturated KCl) electrode was used as a reference electrode instead. Prior to each experiment, all solutions were purged with nitrogen gas, but the solution containing SDS was not because of bubbles generated during the purging process.

Preparation of Conducting Polymer Films. Conducting polymer films were electrochemically prepared. The PPy film was grown galvanostatically by applying 1.0 mA (=3.92 mA/cm^2) for 10 s in an acetonitrile solution containing 1% water, 0.10 M pyrrole, and 0.10 M $LiClO_4$.[16b] The P3MeT film was grown potentiostatically by applying 1.8 V for 10 s in a propylene carbonate solution containing 0.10 M 3MeT and 0.50 M $LiClO_4$.[17] The PEDOT films were grown potentiostatically by applying 1.0 V for 10 s in aqueous solutions containing 0.030 M EDOT, 0.10 M $LiClO_4$ and 0.050 M SDS or in nonaqueous solutions without SDS. SDS was used as an anionic surfactant to increase the solubility and also to reduce the oxidation potential of EDOT in water. Because of bubbles generated during the purging process, the dodecyl sulfate (DS^-) doped PEDOT film was grown immediately after the solution was prepared. After electropolymerization, the films were rinsed with the solvent to clean the surface of polymer films and dried under vacuum at room temperature.

Preparation of Conducting Polymer−Noble Metal (Pt, Au, Ag) Composites. The Pt nanoparticles were deposited on a pre-synthesized PPy film in a 0.50 M H_2SO_4 solution by electrochemically reducing 1.0 mM K_2PtCl_6 for 3 s at a constant potential more negative than the open circuit potential (OCP), which was 0.5 to ~0.6 V depending on the state of the PPy film, by −0.1 V. The Au or Ag nanoparticle-dispersed composites were produced by simply immersing the polymer films into colloidal solutions containing Au or Ag nanoparticles for a prescribed duration (5 to ~10 min). The commercially available Au colloid solution containing gold particles of 20 nm[21] or a homemade Ag colloid solution prepared simply by mixing 0.25 mM $AgClO_4$ and 0.50 mM $NaBH_4$ in an aqueous solution with vigorous stirring at room temperature were used as the sources of nanoparticles of Au or Ag.[22]

Characterization. A field-emission scanning electron microscopy (FE-SEM, Philips, XL30SFEG) equipped with an energy dispersive X-ray (EDX) module was used to confirm the nanoparticles and to perform elemental analysis. The contact mode AFM with a current-sensing module (i.e., current-sensing AFM (PicoSPM, Molecular Imaging Inc.))[23] was used to obtain not only the current and friction images but also current−voltage ($I-V$) curves at selected sites of the current image. Platinum−iridium (PtIr) coated cantilevers (spring constant, 0.16 to ~0.20 N/m) were used for imaging the Pt dispersed composites and obtaining all $I-V$ traces at the points of the particles on polymer surfaces during the AFM scan. The conductive diamond coated cantilevers (spring constant, 0.17 to ~0.21 N/m) were used for imaging Au and Ag dispersed composites. All cantilevers used were purchased from Nanosensors. The load force was maintained at 7 to ~9 nN to avoid the damage of the tip and the sample. A bias voltage between the substrate (Au) and the conducting cantilever, which was grounded, was adjusted depending on situations during the imaging experiments. Before imaging a nanocomposite surface, the surface was purged with the high purity N_2 gas, and all the AFM experiments were carried out under a nitrogen atmosphere to minimize the effects of moisture and adsorbed water. To obtain reliable point-contact $I-V$ measurements at noble metal islands connected to conducting polymer films, the load force was frequently checked to see if the desired force was maintained during the AFM scan.

Results and Discussion

Pt Particles on PPy Films. The Pt nanoparticles were deposited by electrochemically reducing K_2PtCl_6.[24] To find an optimal experimental condition for Pt electrodeposition on the PPy fims, we examined effects of various experimental parameters including the reduction potential, the concentration of K_2PtCl_6, and the deposition time with a fixed thickness of the PPy film. By varying these parameters, it was possible to control the particle size and the distribution of Pt particles to some extent, and the best results were obtained by electrochemically depositing Pt particles at a constant potential more negative than the OCP (0.5 to ~0.6 V) by −0.10 V for 3 s in a 0.5 M H_2SO_4 solution containing 1.0 mM K_2PtCl_6 on a pre-synthesized PPy film (hereafter denoted as Pt/PPy); this procedure was used only for the deposition of Pt nanoparticles on the conducting polymer matrix.

Figure 1 shows a SEM (a) and the corresponding EDX spectrum (b) obtained for the Pt nanoparticles electrodeposited on the PPy film galvanostatically grown at a glassy carbon electrode; the glassy carbon electrode was used instead of the gold-on-silicon substrate for the EDX elemental analysis to avoid the overlap of energy peaks generated from Pt particles and the gold electrode. The SEM image shows that Pt particles are reasonably well-dispersed on the PPy film and that the corresponding EDX spot analysis (Figure 1b) identifies that the particles are platinum. As can be seen, the Pt atoms form relatively large aggregates of tens of nanometers and have a rather large size distribution. Significant efforts have been made to control the particle size and the dispersion by manipulating the experimental factors through electrochemical methods.[24]

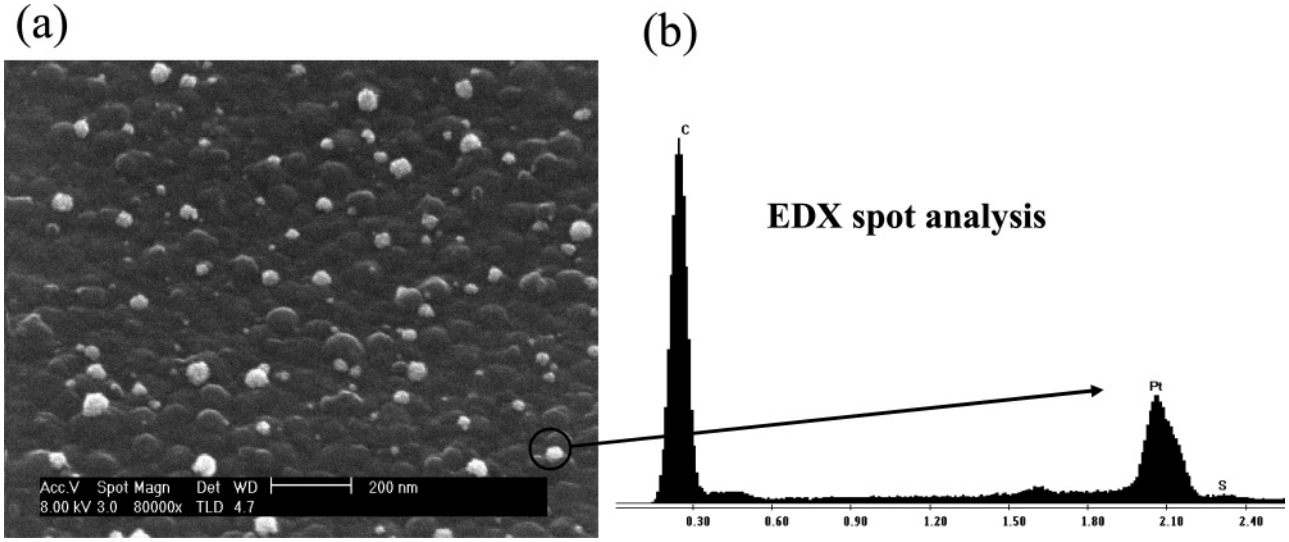

Figure 1. (a) SEM image of Pt nanoparticles deposited on doped PPy film and (b) corresponding EDX spectra. Platinum particles were cathodically deposited by applying a constant potential that was more negative than the OCP by −0.10 V for 3 s in an aqueous solution containing 1 mM K_2PtCl_6 and 0.50 M H_2SO_4.

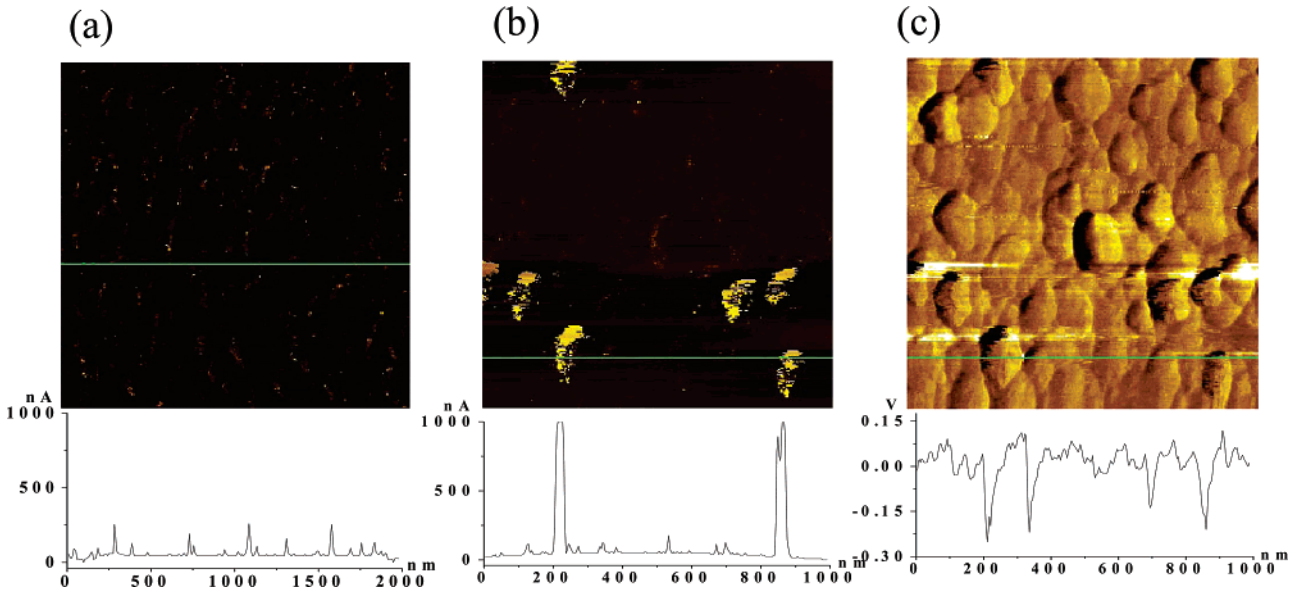

Figure 2. (a) Current image recorded for a PPy film after it was subjected to the same experimental conditions as for Figure 1a in an electrolyte solution without the platinum precursor $PtCl_6^{2-}$ and (b) the current and (c) the friction images concurrently recorded for the same Pt/PPy film as was used in Figure 1. The first current map shown in panel a was used as a reference image for comparison with that of Pt/PPy film shown in panel b. The scan area of all AFM images is 1 μm × 1 μm.

However, controlling the particle sizes and their distribution was not very straightforward, and the one shown here represents just about the best example.

Having confirmed the identities of Pt particles on the polymer surface from the SEM image and the EDX analysis, we now ran CS-AFM experiments. Figure 2 shows the current images of the PPy film subjected to identical experimental conditions as for the electrodeposition of Pt particles in aqueous solutions without (a) and with (b) the platinum precursor ($PtCl_6^{2-}$) present, along with a simultaneously obtained friction image (c) for the identical Pt/PPy film used for Figure 1. Here, the image shown in Figure 2a serves as a reference for comparison with that shown in Figure 2b. A bias potential between the substrate and the conducting tip was very small at 0.20 mV during the CS-AFM experiment. The current map in Figure 2a shows that small currents (bright spots) flow throughout the film. This results from the fact that the PPy film is slightly dedoped while Pt particles are being electrochemically deposited, for which reductive conditions have been used to electrochemically deposit Pt particles. On the other hand, the current image shown for the Pt/PPy film (Figure 2b) reveals that there are bright spots (high current flowing) of globular shapes (compare with the image shown in Figure 2c), which are not shown in Figure 2a. The cross-sectional profile displayed below the current image in Figure 2b also shows that currents of higher than 1.0 μA are flowing at bright spots; the maximum value our amplifier can handle is 1.0 μA at the bias potential of only 0.20 mV. These observations indicate that the bright spots are Pt nanoparticles electrodeposited on the PPy surface; they not only have good contacts with the PPy film but also show significantly higher currents flowing at the particles. Two reasons why much higher currents flow at Pt islands are that (1) the electron transport is facilitated when the conducting tip is in contact with Pt particles during AFM scanning due to a larger contact area between the metal and the polymer, which reduces the contact resistance and (2) the PPy film underneath the Pt islands is not as

efficiently dedoped as for the other areas even after the film was briefly subjected to the reductive environment for electrodeposition of Pt. The tip/polymer contact experiences a large resistance to the current flow due to a small contact area between the tip and the polymer, while the contact through the nanoparticles would present a much smaller resistance leading to larger currents. This can be seen from the equation

$$R = \frac{1}{\kappa}\frac{l}{A} \tag{1}$$

where κ is the conductivity of the film, l is the thickness of the film, and A is the contact area between the tip or the nanoparticle and the film. This equation indicates that the resistance is inversely proportional to the contact area for a given conductivity and film thickness. The contact area between the tip and the film depends on the loading force of the tip as well as the elasticity of both the tip and the film, which can be computed using the Hertz theory expressed by the following equation:[25]

$$a^3(F) = \frac{3}{4}\frac{R^*(F + F_{ad})}{E^*} \tag{2}$$

where F is the external loading force (=9 nN), F_{ad} is the adhesion force ($\cong$1 nN), R^* is an effective radius of curvature of the tip−sample system with $1/R^* = (1/R_{tip}) + (1/R_{sample})$, where R_{sample} is the radius of the sample, resulting in $R^* \approx R_{tip} = 10$ nm; and E^* is the effective Young's modulus with $1/E^* = (1 - \sigma_t^2)/E_t + (1 - \sigma_s^2)/E_s$, where E_t and E_s are Young's modulus of the tip ($E_t = 168$ GPa) and the sample ($E_s = 1.1$ (PPy), 3.2 (PEDOT) GPa[26]), and σ_t (0.38) and σ_s (0.38) are the corresponding Poisson ratios.

The contact areas we calculated were about 14.5 nm^2 for PPy and 23.4 nm^2 for PEDOT under the experimental conditions used here. On the other hand, the contact area for the particle shown in Figure 2b is calculated to be about 1260 nm^2 for a particle size of ~40 nm in diameter assuming a simple flat, two-dimensional contact, where the contact area is simply πr^2 (r = radius). However, if a half of the spherical particle is buried under the polymer layer, the contact area can be as large as about 5020 nm^2 as the contact area would be ~1/2 of the total area of the sphere ($= 4\pi r^2$), and thus, the resistance would become smaller at ~1/80 or 1/340 of that measured at the tip, leading to a large current as shown in Figure 2b. Also, the dedoping process should have been relatively inefficient underneath the Pt particles due to the difficulty of ejecting the counter anions during the reductive experiments.

We can also see the presence of Pt particles from the comparison of current and deflection images. From the topographical (deflection) images (not shown), it was difficult to distinguish spherical Pt particles from those of the PPy film itself because the PPy film also has a large globular-shaped morphology, which is typical, although their sizes and shapes could be different depending on the growth conditions.[27,28] On the other hand, the friction image shown in Figure 2c provides a fairly clear picture of the globular structure of the Pt particles.

One might also doubt if the Pt particles could possibly be in direct contact with the gold substrate electrode due to its penetration during deposition, and much higher currents may flow as a result of the direct contact; it has been reported that the particles could be distributed in three-dimensional arrays within the polymer layer due to its porosity, when the platinum particles were cathodically deposited on the pre-synthesized PPy film.[29] Thus, we fully reduced the Pt/PPy film to verify the point; the film, which had been used in Figure 2, was fully dedoped

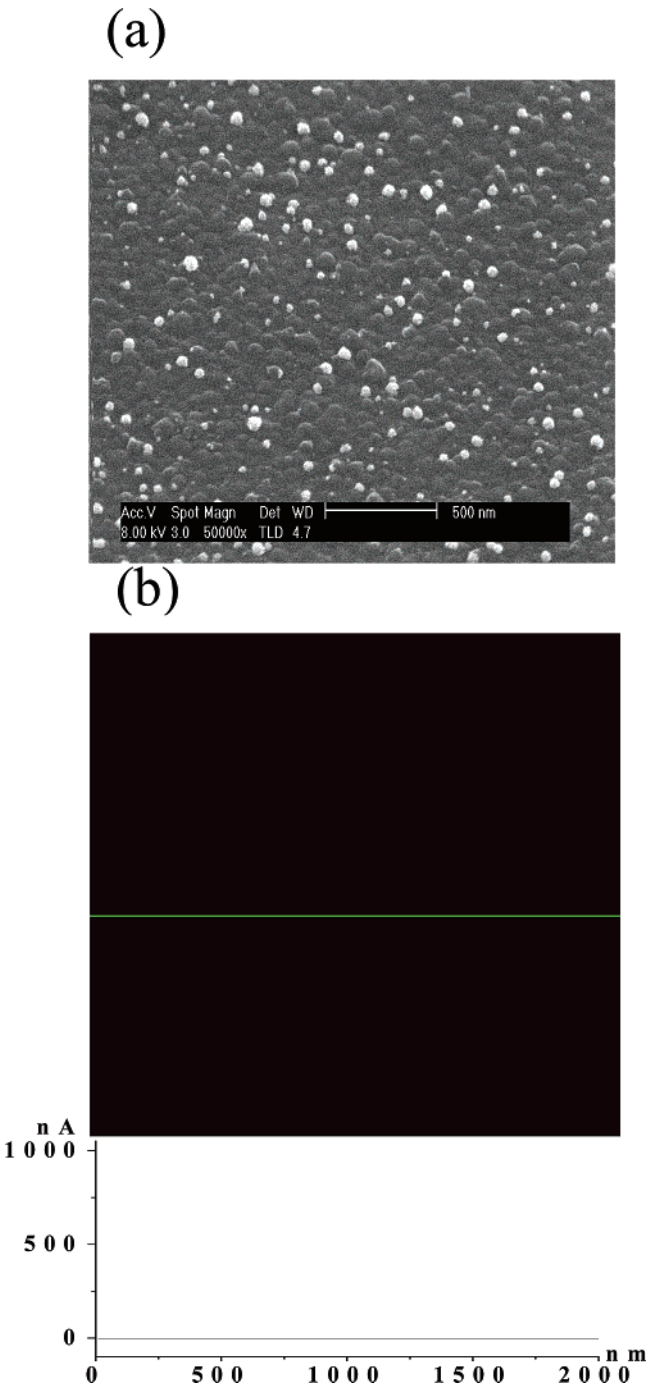

Figure 3. (a) SEM and (b) current images of a fully dedoped Pt/PPy composite after reducing for 5 min at −0.50 V more negative than the OCP in a 0.1 M $LiClO_4$ ACN solution with no water and pyrrole monomers. The scan area of two images is 2 μm × 2 μm.

by electrochemical reduction for a lengthy period until no further cathodic current flowed. Figure 3a shows its SEM image and Figure 3b the current image recorded from it. As can be seen from the cross-sectional profile, almost no currents flow over the entire area even though the Pt nanoparticles are present on the surface (Figure 3a). If Pt particles were directly in contact with the gold substrate, the regions where high currents flow would have remained in the current image even after thorough dedoping. The lack of the bright spots in the current image indicates that the film is fully reduced and that the Pt particles are dispersed on the surface of the PPy film without penetrating into the bulk of the polymer film. Another evidence is that the bright spots in the current image were observed consistently at

the sites where the nanoparticles are located even though the film thickness was increased from that shown in Figure 2 (110 nm) to as thick as 310 nm by increasing the reaction time for the potentiostatic deposition of the PPy film.

Au Particles Dispersed on Polymers of Thiophene Derivatives. These composites were obtained by an extremely simple procedure. In general, it is well-known that gold (Au) can easily form a chemical bond with sulfur atoms as has been demonstrated widely during the studies of self-assembled monolayers of not only alkyl thiols[30] but also thiophene and its derivatives[31] on gold electrodes. Thus, we expect that the surfaces of conducting polymer films prepared by electropolymerization of an electroactive monomer containing a sulfur atom in its heterocyclic structure would interact strongly with the Au nanoparticles and form rather good contacts on the nanoscale via chemical bonding. To prepare the Au particle-dispersed polymer films, the conducting polymer films were electrochemically synthesized on a substrate electrode first and washed thoroughly with the same solvent as used for their preparation, followed by further washing with deionized water and the solvent by turns a few more times to remove any impurities including monomer or oligomer molecules as well as excess supporting electrolytes. The films thus prepared were then immersed in an Au colloid solution for a specified duration. The commercially available Au colloid solution with gold particles of a diameter of an average of 20 nm was used for the experiments. After taking the films out of the colloid solution, they were thoroughly rinsed with deionized water once more to wash off the physically adsorbed particles on the polymer surface as much as possible. Then, we examined the surface of the polymer film by using scanning electron microscopy to confirm whether Au nanoparticles were actually deposited on the surface or not.

Figure 4 shows SEM images of a variety of conducting polymer films: PPy (a), P3MeT (b), and PEDOT (c) after immersing into the Au colloid solution; we included the PPy film for comparison with the polymers of thiophene derivatives. While a couple of Au particles are seen on the PPy film although the film was dipped in it for an hour (Figure 4a), polymers of thiophene derivatives show a large number of particles of exactly 20 nm in size deposited all over the surface, although the films have been dipped for only 5 min. In other words, there are almost no interactions between the surface of the PPy film and the Au particles, whereas Au particles are successfully drawn onto the surfaces of polymers of thiophene derivatives. This means that the chemical bonding is predominant during the deposition of Au nanoparticles as has been reported for their monomers,[31] although the physical adsorption may not be completely ruled out.

Now that we have confirmed Au nanoparticles chemically bonded to the surface of P3MeT and PEDOT by taking SEM images, the electronic transport properties between them have also been investigated on the nanoscale by the CS-AFM as well. First, the Au nanoparticle-deposited PEDOT (Au/PEDOT) film has been examined, and the results are shown in Figure 5. Figure 5a shows the current image of an as-prepared PEDOT film, and Figure 5b,c show current and friction images concurrently recorded from a different part of the same Au/PEDOT film as used for Figure 4b,c. Here, the image shown in Figure 5a is used as a reference for comparison with that of the Au/PEDOT film shown in panel b. A bias voltage between the substrate and the conducting cantilevers was 0.20 V. For these imaging experiments, we used a conductive boron-doped diamond (BDD) coated cantilever instead of a metal coated one. When metal

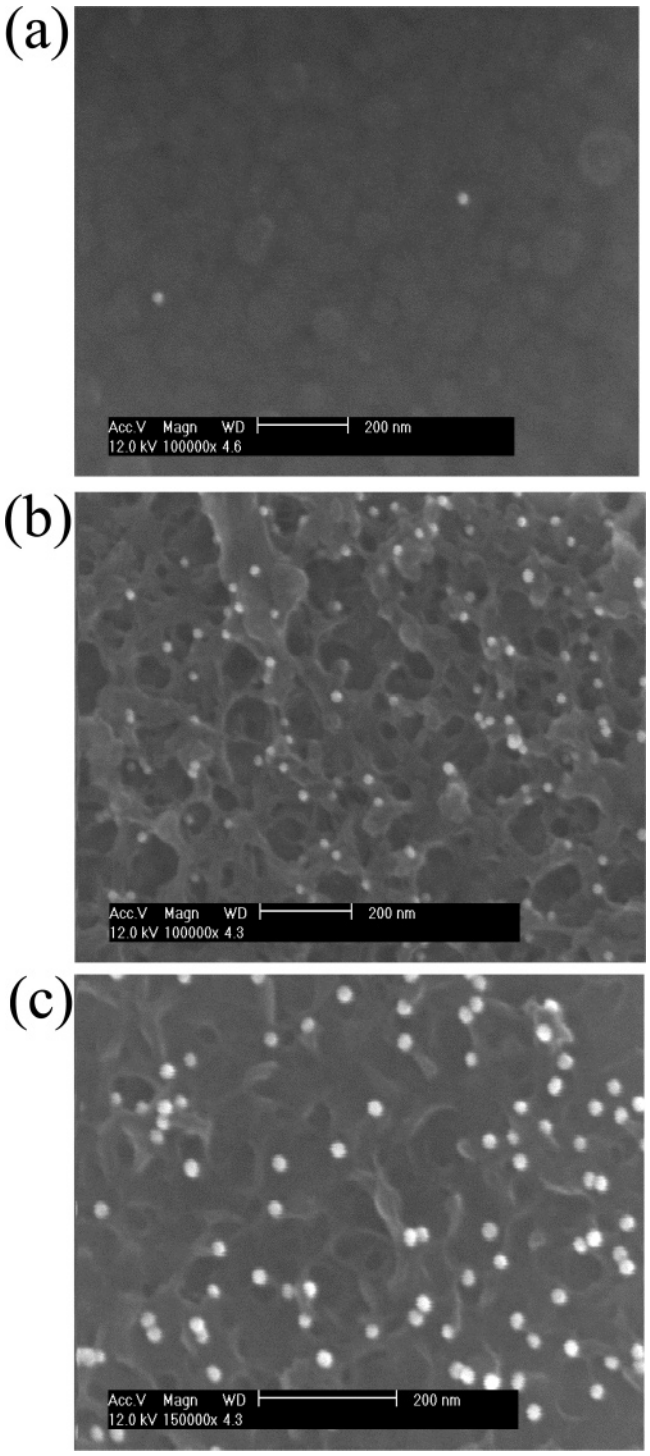

Figure 4. SEM images obtained for the surface of various conducting polymer films after they were dipped into the Au (20 nm) colloid solution: (a) PPy, (b) P3MeT, and (c) PEDOT. Dipping time was 1 h for PPy, while it was 5 min for both P3MeT and PEDOT films.

coated cantilevers were used, the currents were so high that they were easily saturated at our current sensitivity for the as-grown PEDOT film, which is in a doped state, even at a small bias potential, and we were not able to see the differences in current for one sample from another. Furthermore, AFM images were often distorted during imaging, showing a number of scratched areas. Thus, it was rather difficult to distinguish Au islands from the polymer film itself and obtain reasonably clear AFM images. On the other hand, we were able to acquire clearer images when BDD tips were used and also lower the current sensitivity considerably from the saturation level because the tips them-

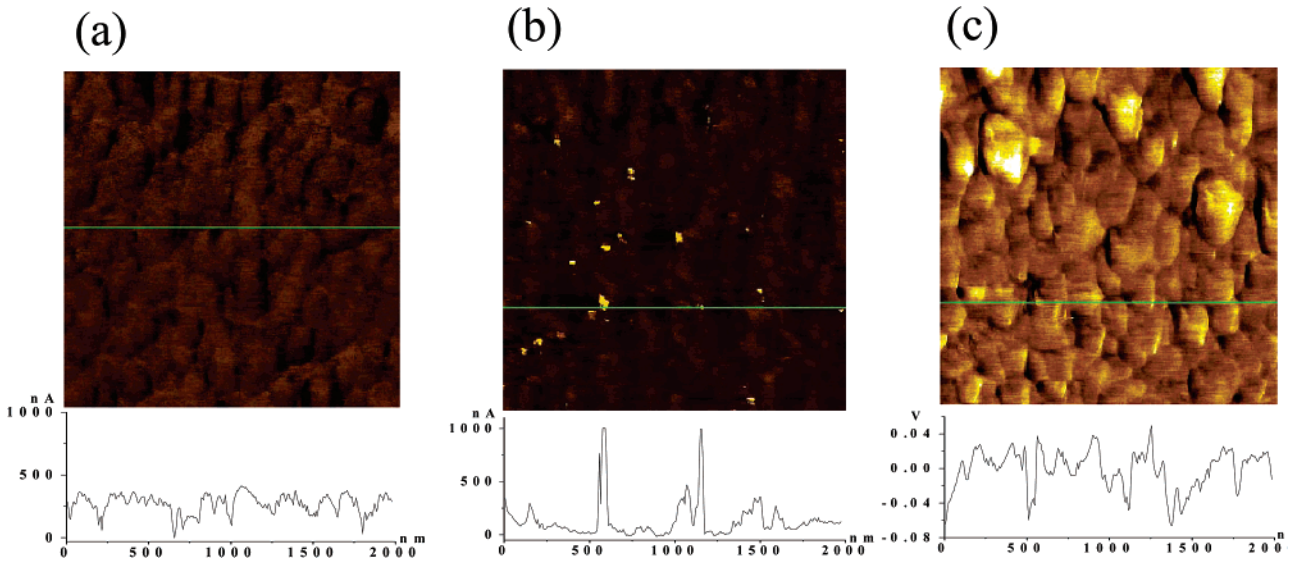

Figure 5. Current image of an as-grown PEDOT film (a) and simultaneously obtained current (b) and friction (c) images for the same Au/PEDOT as used for Figure 4c. The scan area is 2 μm $\times$ 2 μm.

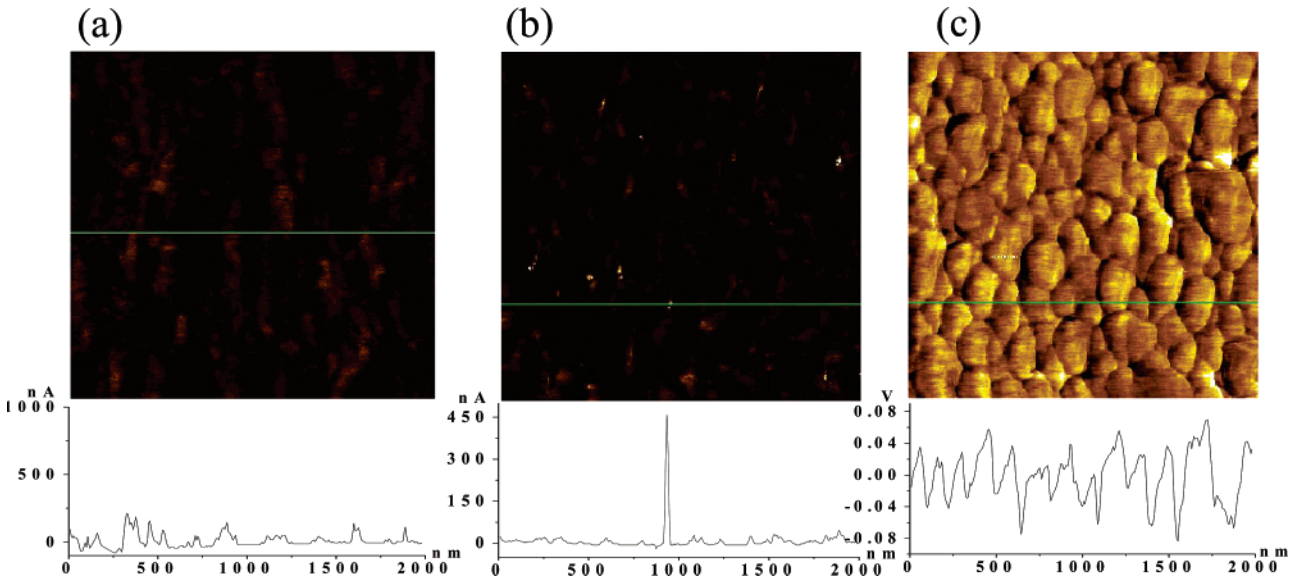

Figure 6. Current image of an as-prepared P3MeT film (a) and simultaneously obtained current (b) and friction (c) images for Au/P3MeT. The scan size of all AFM images is 2 μm $\times$ 2 μm.

selves were significantly less conductive than noble metal coated cantilevers. For this reason, some Au particles are not seen as clearly as those shown in the Figure 4b,c.

The current map of the as-grown PEDOT film shown in Figure 5a demonstrates that currents flow relatively homogeneously over almost the entire surface with almost no high current flowing areas at the bias of 0.20 V, whereas the current image recorded from the Au/PEDOT composite shown in Figure 5b exhibits bright spots with maximum currents up to 1.0 μA at the same bias voltage; this is also fairly clearly seen from the comparison of their cross-sectional current profiles displayed below the current images. We believe these are Au nanoparticles bound chemically to the surface of the polymer film. This is also supported by the fact that the slightly protruding regions in the friction image (Figure 5c) correspond to bright spots in the current image (Figure 5b). In the case of 2 μm $\times$ 2 μm images shown in Figure 5b,c, the matches between the two images are not as easily identified as for some other cases. We also observed essentially the same results from PEDOT films prepared in nonaqueous media except that the currents were generally higher than those prepared in aqueous media. This suggests indirectly that PEDOT films have similar surface characteristics regardless of the media, in which they are prepared, although the doped PEDOT film might have undergone some degradation reactions on its surface when prepared in aqueous media.

Likewise, we have investigated Au nanoparticle-deposited P3MeT (Au/P3MeT) films under the same experimental conditions. Figure 6 shows a 2 μm $\times$ 2 μm current image of the as-grown P3MeT film (a) and current (b) and friction (c) images simultaneously obtained for the same Au/P3MeT film as that used for Figure 4b. The bright spots shown in Figure 6b are Au particles on P3MeT, at which higher currents flow. However, unlike the case of the Au/PEDOT film, the cross-sectional profile displayed underneath the current image shown in Figure 6b shows that maximum currents flowing are less than 500 nA, which is about a half of those flowing at Au islands on the Au/PEDOT film (Figure 5b). This indicates that the PEDOT film is more conductive at the sites where particles are sitting than the P3MeT film is. It appears that PEDOT has sulfur atoms on a better aligned surface, and perhaps, more sulfur atoms are bonded to a given area of the Au nanoparticles. We thus

conclude that PEDOT forms a stronger bonding with Au particles, although the PEDOT film could also be more conductive than the P3MeT film.

Ag Particle Dispersed Composites. In efforts to reaffirm whether the same phenomena as observed for the case of the Au particles would be observed for silver (Ag) also, the Ag nanoparticles were examined for the formation of composites. A colloid solution containing Ag nanoparticles that has a size distribution of roughly 10−30 nm under our experimental conditions was produced simply by adding $NaBH_4$ used as both a reductant and a stabilizer to a solution containing $AgClO_4$[22] because the solution was not commercially available. Then, conducting polymer films electrochemically grown were dipped into the Ag colloid solution thus prepared for a specified duration. The SEM image and EDX elemental analysis (not shown) showed that Ag particles were bonded onto the surface of both PEDOT and P3MeT, whereas Ag nanoparticles were not present on the PPy film as was the case for gold nanoparticles. With the composites thus prepared, we obtained current images under the identical conditions to those used for the Au particle-dispersed composites. As expected, the results obtained were very similar to those obtained from the Au particle-dispersed composites and corroborated our observations very well. We will not repeat the description of the same observations here; we only display current (a) and friction (b) images recorded from the Ag-dispersed PEDOT (Ag/PEDOT) film in Figure 7. As can be seen, bright spots with full-scale currents of 1.0 μA are found in the current images in Figure 7a, indicating that these are Ag nanoparticles.

***I*−*V* Measurements at Noble Metal Islands.** Current−voltage (*I*−*V*) characteristics were obtained to evaluate the nature and the degree of the electrical contacts at the point of a particle connected to the polymer film. The measurements were made by scanning the voltage from −1.0 to +1.0 V at a metal island with a Pt−Ir coated tip as shown in Figure 8a; the load force was maintained at 7 to ∼9 nN to obtain reliable results. It is seen in these traces that the currents are saturated in higher voltage ranges. We thus show expanded *I*−*V* curves plotted between −0.10 and +01.0 V in Figure 8b at the points of (1) a Pt nanoparticle electrodeposited on the surface of the PPy film, (2) Ag, and (3) Au nanoparticles on the PEDOT film surface, where the range of the *x*-axis is adjusted appropriately to see all the curves. The particles sizes were 60 to ∼70, 20 to ∼30, and 20 nm in diameter, respectively, for the Pt, Ag, and Au particles. The *I*−*V* traces were linear in the voltage range of −1.0 to +1.0 V, and only expanded versions in the voltage range of ±0.10 V are shown for better resolution. As can be seen, all of these curves have large slopes. The slope of the line for Pt−PPy is the steepest among these. This is because the contact area was the largest for the Pt−PPy contact (∼5650 nm^2), which is followed by the Ag (∼980 nm^2) and the Au particles (∼630 nm^2). The fact that linear *I*−*V* relations are observed indicates that the contacts between the particles and the polymer surfaces are ohmic. Also, the resistances calculated from the slopes of these *I*−*V* curves were 8230, 42 700, and 48 800 Ω, respectively, for the contacts examined in Figure 8a−c. The bulk resistances of the polymer films calculated by dividing the bias voltage by an average current taken at 256 points across 1 μm of the film surface in the current profiles shown underneath the current images and normalized with respect to the contact areas between the nanoparticles and the polymer were 1720, 20 700, and 20 700 Ω, respectively, for the PPy and PEDOT films with no metal particles present under otherwise identical experimental conditions. In other words, the

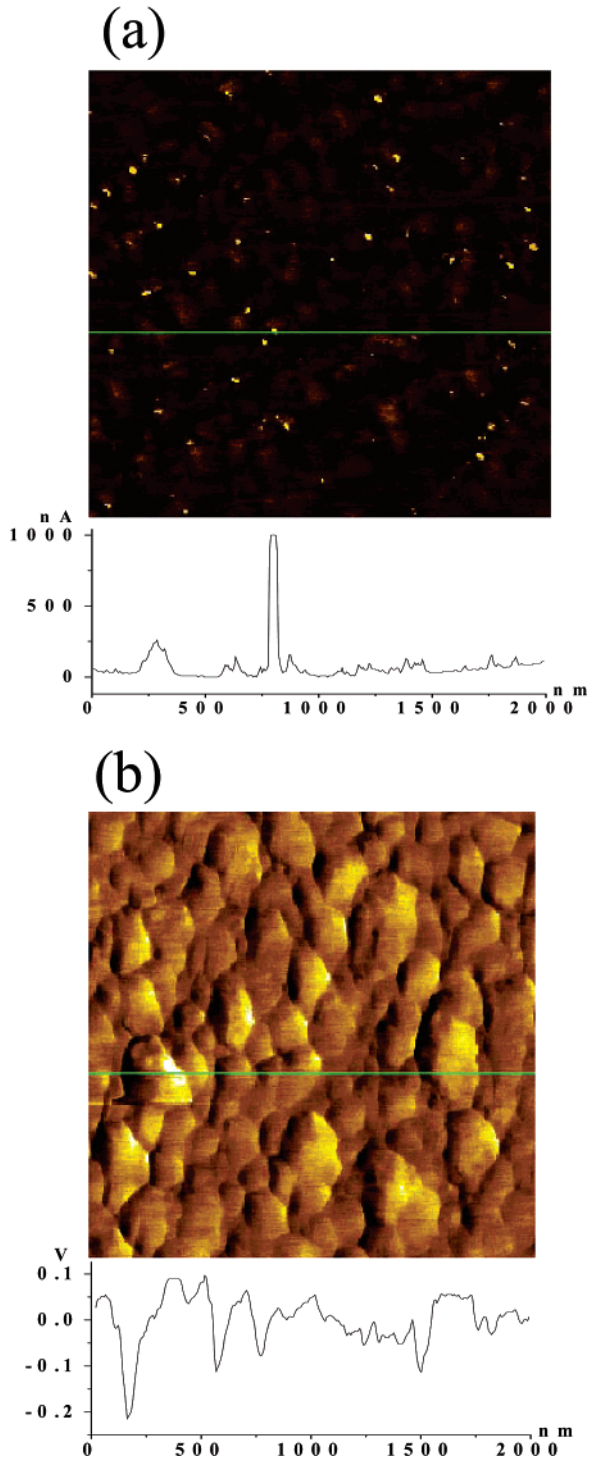

Figure 7. Current (a) and friction (b) images recorded from Ag/PEDOT composites and their cross-sectional analyses. The scan size was 2 μm × 2 μm.

contact resistance between the polymer film and the particle is about 2−5 times the bulk resistance for the case of PPy, while it is about twice for PEDOT. It should be pointed out that we used the smallest possible areas for normalizing with respect to the bulk conductivities. These results show that the contact resistances are larger than the bulk resistances and also that the contacts between gold or silver particles and PEDOT are better than that between platinum and PPy. Even though the contact resistance is smaller than the bulk resistance, the contact is ohmic as long as the *I*−*V* relations are linear; *I*−*V* relations like those typically observed from semiconductor junctions or

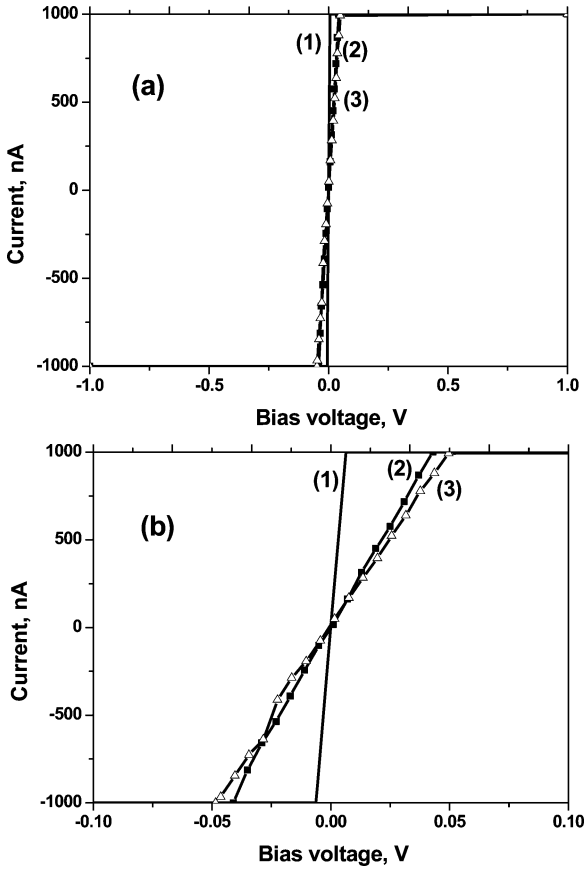

Figure 8. Current−voltage curves obtained in (a) a voltage range of −1.0 to approximately +1.0 V and (b) their expanded versions in a potential range of −0.10 to +0.10 V on (1) a platinum particle electrochemically deposited on PPy film and (2) silver and (3) gold nanoparticles on a PEDOT film, respectively. The Pt−Ir coated tip was used for all $I-V$ measurements.

even those of Zener diodes have been reported for conducting polymer films when the doping level was in a correct range.[17a]

As pointed out previously, the major reason for a larger slope for the PPy−Pt contact is due to the larger contact area. Another reason could be because the PPy film underneath the Pt particles was fairly well-protected in the electrochemical environment during the short period of cathodic reduction, whereas the as-prepared P3MeT and PEDOT films, which are fully doped or oxidized by the time they were prepared, might have formed passive functionalities[32] with water on the surface while the films were dipped in Au and Ag colloid solutions in air. Further, these films might have sulfur oxides formed during their growth in aqueous media. In fact, this could be why the P3MeT and PEDOT films shown in Figures 5a and 6a appear less conductive than that of PPy as shown previously and also than those of as-prepared PEDOT films in nonaqueous media.[17b] Another possibility is the formation of local fuel cells formed at the points where Pt particles are in contact with the PPy film, in which the PPy film becomes oxidized (i.e., doped) as a fuel underneath the Pt particles, while oxygen is reduced on the metal surfaces. This internal fuel cell reaction would keep the PPy film underneath the Pt particles in a better doped state, making it more conductive. The reaction is thermodynamically favorable, as a cell voltage of about 1 V is calculated from the reduction potential of oxygen and the oxidation potential of PPy. Note that Pt is a much better electrocatalyst than Au for oxygen reduction.

Conclusion

In this study, we have demonstrated using CS-AFM that an electrical contact can be successfully established between noble metal nanoparticles and polymer surface and that the interaction of the particles with conducting polymer films can be either physical or chemical. Also, we have shown for the first time that Au and Ag nanoparticles can be easily deposited on the surface of conducting polymer films with sulfur atoms on their heterocyclic rings (P3MeT and PEDOT) containing sulfur, resulting in formation of nanocomposites, just by dipping the films into colloidal solutions containing nanoparticles of gold or silver for a relatively short period (5 to ∼10 min). This results from chemical bonding between metal particles and sulfur atoms on the surface of the polymer film.[31] Of the two polymers prepared from thiophene derivatives, PEDOT turned out to be more conductive at the sites where the particles are sitting on the surface. It appears that PEDOT has sulfur atoms on a better aligned surface owing to its structural characteristics of the monomer and is thus strongly bonded to these metal nanoparticles.

The current−voltage curves obtained at the metal nanoparticle sites indicate that the contacts between the particles and the polymer surfaces are ohmic. This has been an important question for those wanting to use conducting polymers as a substrate for electrocatalysts for fuel cells as well as for electronic devices, particularly for nanostructures. Also, the successful deposition of the Au and Ag nanoparticles by dipping polymer films in a colloidal solution containing their nanoparticles indicates that the intermixed nanocomposites can also be prepared straightforwardly by alternating the polymer growth and dipping into the colloid solution or by growing conducting polymer films in a solution containing both the nanoparticles and the monomer. The gold and silver nanoparticles may also find applications in easier identification of sulfur containing conductive polymer nanodots[33] or nanowires[34] by a simple exposure to their colloidal solutions, followed by SPM examinations.

Acknowledgment. This work was supported by the National R&D Project for Nanoscience and Technology, a research grant from KOSEF through the Center for Integrated Molecular Systems (Grant R11-2000-070-070010), and the BK21 program of the Korea Research Foundation.

References and Notes

(1) (a) Aviram, A. *Chem. Phys. Lett.* **1974**, *29*, 277. (b) Park, J.; Pasupathy, A. N.; Goldsmith, J. I.; Chang, C.; Yaish, Y.; Petta, J. R.; Rinkoski, M.; Sethna, J. P.; Abruna, H. D.; Mceuen, P. L.; Ralph, D. C. *Nature* **2002**, *417*, 722. (c) Park, H.; Park, J.; Lim, A. K. L.; Anderson, E. H.; Alivisatos, A. P.; Mceuen, P. L. *Nature* **2000**, *407*, 57. (d) Liang, W.; Shores, M. P.; Bockrath, M.; Long, J. R.; Park, H. *Nature* **2002**, *417*, 725. (e) Wada, Y. *Ann. N.Y. Acad. Sci.* **2002**, *960*, 39.

(2) Pease, A. R.; Jeppesen, J. O.; Stoddart, J. F.; Luo, Y.; Collier, C. P.; Heath, J. R. *Acc. Chem. Res.* **2001**, *34*, 433.

(3) (a) Tans, S. J.; Verschueren, A. R. M.; Dekker, C. *Nature* **1998**, *393*, 49. (b) Appenzeller, J.; Knoch, J.; Martel, R.; Derycke, V.; Wind, S. J.; Avouris, P. *IEEE Trans. Nanotechnol.* **2002**, *1*, 184. (c) Avouris, P. *Acc. Chem. Res.* **2002**, *35*, 1026.

(4) (a) Lee, J.-O.; Lientschnig, G.; Wiertz, F.; Struijk, M.; Janssen, R. A. J.; Egberink, R.; Reinhoudt, D. N.; Hadley, P.; Dekker, C. *Nano Lett.* **2003**, *3*, 113. (b) Kagan, C. R.; Afzali, A.; Martel, R.; Gignac, L. M.; Solomon, P. M.; Schrott, A. G.; Ek, B. *Nano Lett.* **2003**, *3*, 119.

(5) (a) Singh, R.; Lodha, A. *IEEE Trans. Semiconduct. Mater.* **2001**, *14*, 281. (b) Saxena, V.; Malhotra, B. D. *Curr. Appl. Phys.* **2003**, *3*, 293. (c) Samuel, I. D. W. *Philos. Trans. R. Soc. London, Ser. A* **2000**, *358*, 193. (d) He, H.; Zhu, J.; Tao, N. J.; Nagahara, L. A.; Amlani, I.; Tsui, R. *J. Am. Chem. Soc.* **2001**, *123*, 7730.

(6) Fu, L.; Cao, L.; Liu, Y.; Zhu, D. *Adv. Colloid Interface Sci.* **2004**, *111*, 133.

(7) (a) Nitzan, A.; Ratner, M. A. *Science* **2003**, *300*, 1384. (b) Hipps, K. W. *Science* **2001**, *294*, 536.

(8) (a) Kost, K. M.; Bartak, D. E.; Kazee, B.; Kuwana, T. *Anal. Chem.* **1988**, *60*, 2379. (b) Giacomini, M. T.; Ticianelli, E. A.; McBreen, J.; Balasubramanian, M. *J. Electrochem. Soc.* **2001**, *148*, 323.

(9) (a) Kelley, T. W.; Granstrom, E. L.; Frisbie, C. D. *Adv. Mater.* **1999**, *11*, 261. (b) Gardner, C. E.; Macpherson, J. V. *Anal. Chem.* **2002**, *74*, 576. (c) Park, S.-M.; Lee, H. J. *Bull. Korean Chem. Soc.* **2005**, *26*, 697.

(10) (a) Cui, X. D.; Primak, A.; Zarate, X.; Tomfohr, J.; Sankey, O. F.; Moore, A. L.; Moore, T. A.; Gust, D.; G., H.; Lindsay, S. M. *Science* **2001**, *294*, 571. (b) Cui, X. D.; Zarate, X.; Tomfohr, J.; Primak, A.; Moore, A. L.; Moore, T. A.; Gust, D.; Harris, G.; Sankey, O. F.; Lindsay, S. M. *Nanotechnology* **2002**, *13*, 5. (c) Cui, X. D.; Primak, A.; Zarate, X.; Tomfohr, J.; Sankey, O. F.; Moore, A. L.; Moore, T. A.; Gust, D.; Nagahara, L. A.; Lindsay, S. M. *J. Phys. Chem. B* **2002**, *106*, 8609. (d) Leatherman, G.; Durantini, E. N.; Gust, D.; Moore, T. A.; Moore, A. L.; Stone, S.; Zhou, Z.; Rez, P.; Liu, Y. Z.; Lindsay, S. M. *J. Phys. Chem. B* **1999**, *103*, 4006. (e) Rawlett, A. M.; Hopson, T. J.; Nagahara, L. A.; Tsui, R. K.; Ramachandran, G. K.; Lindsay, S. M. *Appl. Phys. Lett.* **2002**, *81*, 3043.

(11) (a) Wold, D. J.; Frisbie, C. D. *J. Am. Chem. Soc.* **2001**, *123*, 5549. (b) Wold, D. J.; Frisbie, C. D. *J. Am. Chem. Soc.* **2000**, *122*, 2970. (c) Wold, D. J.; Haag, R.; Rampi, M. A.; Frisbie, C. D. *J. Phys. Chem. B* **2002**, *106*, 2813. (d) Beebe, J. M.; Engelkes, V. B.; Miller, L. L.; Frisbie, C. D. *J. Am. Chem. Soc.* **2002**, *124*, 11268. (e) Sakaguchi, H.; Hirai, A.; Iwata, F.; Sasaki, A.; Nagamura, T.; Kawata, E.; Nakabayashi, S. *Appl. Phys. Lett.* **2001**, *79*, 3708. (f) Nakamura, T.; Yasuda, S.; Miyamae, T.; Nozoye, H.; Kobayashi, N.; Kondoh, H.; Nakai, I.; Ohta, T.; Yoshimura, D.; Matsumoto, M. *J. Am. Chem. Soc.* **2002**, *124*, 12642.

(12) (a) Dai, H.; Wong, E. W.; Lieber, C. M. *Science* **1996**, *272*, 523. (b) de Pablo, P. J.; Gomez-Navarro, C.; Martinez, M. T.; Benito, A. M.; Maser, W. K.; Colchero, J.; Gomez-Herrero, J.; Baro, A. M. *Appl. Phys. Lett.* **2002**, *80*, 1462. (c) Li, J.; Stevens, R.; Delzeit, L.; Tee, Ng, H.; Cassell, A.; Han, J.; Meyyappan, M. *Appl. Phys. Lett.* **2002**, *81*, 910.

(13) (a) Alperson, B.; Cohen, S.; Rubinstein, I.; Hodes, G. *Phys. Rev. B* **1995**, *52*, 17017. (b)Alperson, B.; Rubinstein, I.; Hodes, G. *Phys. Rev. B* **2001**, *63*, 81303.

(14) Loiacono, M. J.; Granstrom, E. L.; Frisbie, C. D. *J. Phys. Chem. B* **1998**, *102*, 1679.

(15) (a) Hong, S. Y.; Park, S.-M. *J. Phys. Chem. B* **2005**, *109*, 9305. (b) Han, D. H.; Park, S.-M. *J. Phys. Chem. B* **2004**, *108*, 13921.

(16) (a) Lee, H. J.; Park, S.-M. *J. Phys. Chem. B* **2004**, *108*, 1590. (b) Lee, H. J.; Park, S.-M. *J. Phys. Chem. B* **2005**, *109*, 13247. (c) Han, D. H.; Lee, H. J.; Park, S.-M. *Electrochim. Acta* **2005**, *50*, 3085.

(17) (a) Lee, H. J.; Park, S.-M. *J. Phys. Chem. B* **2004**, *108*, 16365. (b) Han, D.-H.; Kim, J.-W.; Park, S.-M. *J. Phys. Chem. B* **2006**, *110*, 14874.

(18) (a) Jocowitz, H.; Li, M.; Baer, D. R.; Engelhard, M. H.; Janta, J. *J. Electrochem. Soc.* **1995**, *142*, 798. (b) Sargent, A.; Loi, T.; Gal, S.; Sadik, O. A. *J. Electroanal. Chem.* **1999**, *470*, 144. (c) Croissant, M. J.; Napporn, T.; Leger, J.; Lamy, C. *Elctrochim. Acta* **1998**, *43*, 2447. (d) Kern, J.-M.; Sauvage, J.-P. *J. Chem. Soc., Chem. Commun.* **1989**, *657*. (e) Segawa, H.; Shimidzu, T.; Honda, k. *J. Chem. Soc., Chem. Commun.* **1989**, *132*.

(19) (a) Lee, H. J.; Park, S.-M. *Bull. Korean Chem. Soc.* **2005**, *26*, 697. (b) Park, S.-M. *Handbook of Conductive Molecules and Polymers*; Nalwa, H. S., Ed.; Ellis Harwood: Chichester, UK, 1997; Vol. 3.

(20) Sih, B. C.; Wolf, M. O. *Chem. Commun.* **2005**, 3375.

(21) Slot, J. W.; Geuze, H. J. *Eur. J. Cell Biol.* **1985**, *38*, 87.

(22) Van Hyning, D. L.; Zukoski, C. F. *Langmuir* **1998**, *14*, 7034.

(23) Visit, for example, http://www.molec.com.

(24) (a) Holdcroft, S.; Funt, B. L. *J. Electroanal. Chem.* **1988**, *240*, 89 (b) Bose, C. S. C.; Rajeshwar, K. *J. Electroanal. Chem.* **1992**, *333*, 235. (c) Becerik, İ.; Süzer, S.; Kadirgan, F. *J. Electroanal. Chem.* **2001**, *502*, 118. (d) Bouzek, K.; Mangold, K.-M.; Jüttner, K. *Electrochim. Acta* **2000**, *46*, 661.

(25) (a) Isrraelachvili, J. *Intermolecular and Surface Forces*; Academic Press: London, 1992. (b) Riedo, E.; Brune, H. *Appl. Phys. Lett.* **2003**, *83*, 1986.

(26) (a) Bay, L.; Mogensen, N.; Skaarup, S.; Sommer-Larsen, P.; Jorgensen, M.; West, K. *Macromolecules* **2002**, *35*, 9345. (b) Duvail, J. L.; Rétho, P.; Godon, C.; Marhic, C.; Louarn, G.; Chauvet, O.; Cuenot, S.; Nylsten, B.; Dauginer-De Pra, L.; Demoustier-Chempagne, S. *Synth. Met.* **2003**, *135*−*136*, 329.

(27) Ko, J. M.; Rhee, H. W.; Park, S -M.; Kim, C. Y. *J. Electrochem. Soc.* **1990**, *137*, 905.

(28) (a) Sadki, S.; Schottland, P.; Brodie, N.; Sabouraud, G. *Chem. Soc. Rev.* **2000**, *29*, 283. (b) Suarez, M. F.; Compton, R. G. *J. Electroanal. Chem.* **1999**, *462*, 211. (c) Hwang, B. J.; Santhanam, R.; Lin, Y.-L. *J. Electrochem. Soc.* **2000**, *147*, 2252.

(29) Becerik, İ.; Kadirgan, F. *J. Electroanal. Chem.* **1997**, *436*, 189.

(30) Bain, C. D.; Troughton, E. B.; Tao, Y. T.; Evall, J.; Whitesides, G. M.; Nuzzo, R. G. *J. Am. Chem. Soc.* **1989**, *111*, 321.

(31) (a) Dishner, M. H.; Hemminger, J. C.; Feher, F. J. *Langmuir* **1996**, *12*, 6176. (b) Matsuura, T.; Sakaguchi, H.; Shimoyama, Y. *J. Mater. Sci.* **2003**, *14*, 353.

(32) McCulloch, I.; Bailey, C.; Giles, M.; Heeney, M.; Love, I.; Shkunov, M.; Sparrowe, D.; Tierney, S. *Chem. Mater.* **2005**, *17*, 1381.

(33) Lee, J.-Y.; Park, S.-M. *J. Electrochem. Soc.* **2000**, *147*, 4189.

(34) Choi, S.-J.; Park, S.-M. *Adv. Mater.* **2000**, *12*, 1547.